Supporting Information

DNAzyme- and Light-Induced-Driven Dissipative and Gated DNA Networks

Jianbang Wang,‡[a] Zhenzhen Li,‡[a] Zhixin Zhou,[a] Yu Ouyang,[a] Junji Zhang,[b] Xiang Ma,[b] He Tian[b] and Itamar Willner*[a]

[a.] Institute of Chemistry, The Center for Nanoscience and Nanotechnology, The Hebrew University of Jerusalem, Jerusalem 91904, Israel
[b.] Key Laboratory for Advanced Materials and Joint International Research Laboratory of Precision Chemistry and Molecular Engineering, Feringa Nobel Prize Scientist Joint Research Center, School of Chemistry and Molecular Engineering, Frontiers Center for Materiobiology and Dynamic Chemistry, East China University of Science and Technology, Shanghai 200237, P. R. China.

*E-mail: Itamar.willner@mail.huji.ac.il

‡These authors contributed equally to this work.

Materials and Methods

Oligonucleotides were purchased from Integrated DNA Technologies. The Cy5-, Cy3- and BHQ2-labeled oligonucleotides were purified by high-performance liquid chromatography. All the sequences of the oligonucleotides were listed below. The Pb^{2+}-ion-dependent DNAzyme sequence in strand A was underlined and the ribonucleobase cleavage site, rA, in strand T was indicated in bold.

A: 5'-TTGTCTTGACGAAAA*TCCGAGCCGGTCGAAA*AAAAGGAGCACGCTA-3'

B: 5'-TAGTGTGCTCCCCGTCAAGACAA-3'

C: 5'-Cy5-AGGAGCACGCATCTGTTTGT-3'

D: 5'-GTTGCTGGGTCTTGACGG-BHQ2-3'

T: 5'-CTCCTTTTT**rA**GTTTTCGTC-3'

T_c: 5'-CTCCTTTTTAGTTTTCGTC-3'

E: 5'-Cy3-AGGAGCACGCACTGTAGACA-5'

I_1: 5'-ACAAACAGATGCGTGCTCCT-3'

I_2: 5'-TGTCTACAGTGCGTGCTCCT-3'

U_1: 5'-CCATTCAGCGATGTTAGGAGCACGCATCTGTTTGT-3'

U_2: 5'-GTTGCTGGGTCTTGACGGTAACCACCCATGTTTAGCT-3'

U_3: 5'-CTGTTCAGCGATGTTAGGAGCACGCACTGTAGACA-3'

S_1: 5'-FAM-AGCTAAT**rA**GGAATGG-BHQ1-3'

S_2: 5'-Cy5-AGCTAAT**rA**GGAACAG-BHQ2-3'

F_t/F_c: 5'-CC***azo***CC***azo***TT***azo***AC***azo***CC***azo***CA***azo***AAAGGTAGCCTCCTAAGAAAA GG-3'

G: 5'-TTTGGGGTAAGGGGTTTGGGGTAAGGGG-3'

H: 5'-CAACAGACATGGGTGAAGGTCAGATTCCATCCAGATGGGGTAAGGGG TTTGGG-3'

I: 5'-Cy5-CATCTGGATGGAATCTGACCTTCACCCATGTCTGTTG-3'

J: 5'-TTACCCCAAACCCCTTACCCGTCAAGACCCAGCAACTCCCTC-3'

K: 5'-GAGGGAGTTGCTGGGTCTTGAC-BHQ2-3'

F_n: 5'-CCCCTTACCCCAAAAGGTAGCCTCCTAAGAAAAGG-3'

Measurements of the Pb^{2+}-ion-dependent DNAzyme-driven dissipative processes.

Strands A and B were mixed with C and D (0.2 μM each one) at 37℃ for one hour and then were annealed to 33℃ for two hours in 10 mM Tris buffer with 20 mM Mg^{2+} and 100 nM Pb^{2+} (200 μL, pH 7.4). The samples were measured with λ_{ex} = 635 nm and λ_{em} = 665 nm at 33℃ (calibrated with thermometer). After adding the trigger strand T (0.6, 0.8, 1.0 μM), the measurements were performed for about 2.5 ho urs.

For the control experiment, the strand T_c without the ribonucleobase cleavage site was added. For the oscillation process, the trigger T (1 μM) was added at the interval of ca. 2.5 hours. The calibration curve was derived from the measurements of the samples, containing C and D (0.2 μM), with different concentrations of strand B (0, 0.04, 0.08, 0.12, 0.16 and 0.2 μM) to calculate the transient concentrations of the structure B/C+D and C in the samples.

Experiments of the inhibitor-gated two dissipative networks.

The measurements of the gated two dissipative networks were performed with different concentrations of inhibitor I_1 or I_2, respectively, mixed with the samples composed of 0.2 μM AB, 0.2 μM C, 0.2 μM E and 0.4 μM D in 10 mM Tris buffer with 20 mM Mg^{2+} and 100 nM Pb^{2+} (200 μL, pH 7.4). After adding the trigger strand T (1.0 μM), the measurements were performed for about 2.5 hours measuring with λ_{ex1} = 635 nm, λ_{em1} = 665 nm and λ_{ex2} = 545 nm, λ_{em2} = 565 nm.

Measurements of the catalytic reactions of DNAzymes with the inhibitor-gated two dissipative networks.

For the measurements of DNAzymes catalytic reactions, the samples containing 1 μM AB, 1 μM U_1, 1 μM U_3 and 2 μM U_2 (10 mM Tris, 20 mM Mg^{2+}, 100 nM Pb^{2+}, pH 7.4) were prepared with 1 μM I_1 or 1 μM I_2 or none. The samples were taken out 100 μL at different time intervals after adding the trigger strand T (5 μM), and were added with 2 μL of the substrate S_1/S_2 (100 μM) followed with the measurements with λ_{ex1} = 495 nm, λ_{em1} = 518 nm and λ_{ex2} = 635 nm, λ_{em2} = 665 nm at 25℃.

Measurements of the Light-driven dissipative processes.

Azobenzene-modified strand F_t (*trans*-state) (0.8 μM), G strand (0.4 μM) were mixed with H, I strands and J, K (0.2 μM each one) in 10 mM Tris buffer with 20 mM Mg^{2+} (600 μL, pH 7.4). The samples were stabilized at 55℃ for 10 min and then were irradiated with UV light (365 nm, 5 W) for different time (5 and 10 min). The measurements were taken with λ_{ex} = 635 nm and λ_{em} = 665 nm at 55℃ (calibrated with thermometer). During the measurement, the cuvette was sealed with a cap to avoid the evaporation of the sample solution.

For the oscillation processes, the samples (0.8 μM F_t, 0.4 μM G, 0.2 μM HIJK, 600 μL) were irradiated by UV light (365 nm, 5W) for 10 min every 250 min or 750 min. For one control experiment, the sample (0.8 μM F_t, 0.4 μM G, 0.2 μM HIJK, 600 μL) was measured at 25℃ for 750 min after the UV irradiation (365 nm, 5 W, 10 min at 55℃). For the second control experiment, strand F_n was used to substitute strand F_t in the sample (0.8 μM F_n, 0.4 μM G, 0.2 μM HIJK, 600 μL). The sample was irradiated by UV light (365 nm, 5 W) for 10 min and the measurement was taken for 1 hour at 55℃.

The calibration curve was derived from the measurements of the samples, containing H/Cy5-I (0.2 μM), with different concentrations of strand J/BHQ2-K (0, 0.04, 0.08, 0.12, 0.16 and 0.2 μM) to calculate the transient concentrations of structures HIJK and H/Cy5-I in the samples.

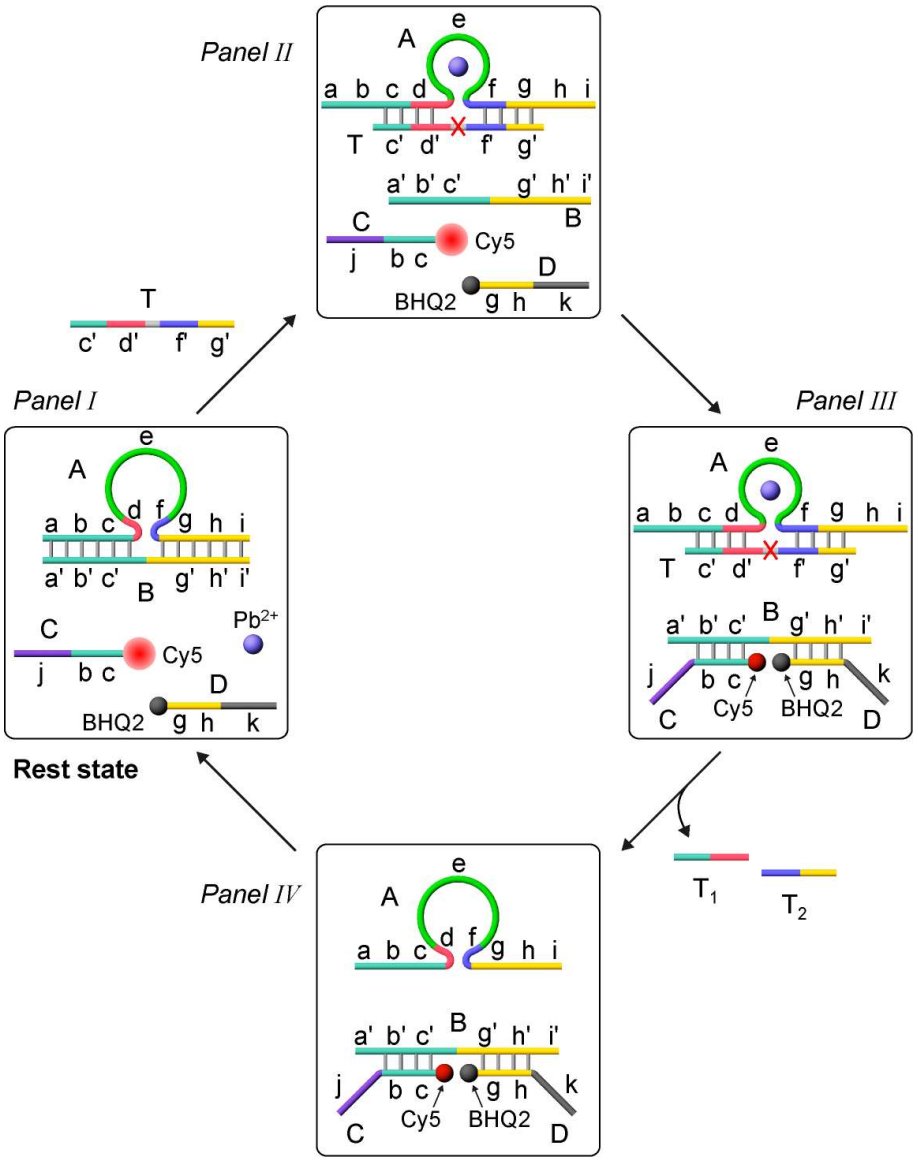

Figure S1. Schematic stepwise operation of the Pb^{2+}-ion-dependent DNAzyme-driven dissipative network. The parent state of the system, Panel I, includes the A/B duplex scaffold as constituent, the Cy5-C and BHQ2-D strands and Pb^{2+} ions. Subjecting the system to the fuel-trigger T results in the displacement of strand B, and the formation of the duplex A/T where the loop domain of A binds the Pb^{2+} ions, and the ribonucleobase-containing strand T acts as substrate of the resulting supramolecular Pb^{2+}-ion-dependent DNAzyme, Panel II. The strand B binds, through hybridization, with the strands Cy5-C and BHQ2-D and forms the intermediate product B/Cy5-C+BHQ2-D and the biocatalytic structure A/T, Panel III. The strand T is being cleaved resulting in the "waste" products T_1+T_2 and the released strand A, Panel IV. The displacement of the strand B from the network product B/Cy5-C+BHQ2-D by A recovers the parent system, Panel I. The dissipative process is followed by the transient time-dependent fluorescence changes generated by the B/Cy5-C+BHQ2-D module.

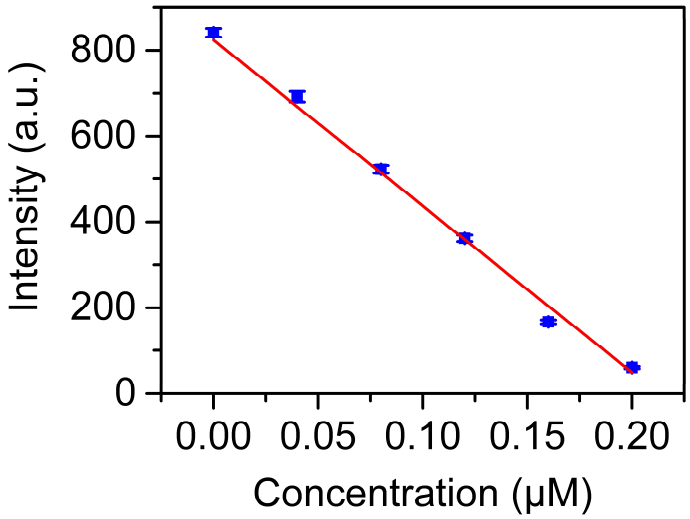

Figure S2. Calibration curve corresponding to the fluorescence intensities of a mixture of Cy5-C and BHQ2-D (each 0.2 μM) in the presence of variable concentrations of the strand B. The curve is fit linearly and the r^2 = 0.98826. The calibration curve provides a quantitative relation between the fluorescence intensity of the B/Cy5-C+BHQ2-D module and its molar concentration. The calibration curve provides a means to translate the fluorescence changes of the dissipative system into quantitative transient concentration changes of the reaction products B/Cy5-C+BHQ2-D along the dissipative transient operation of the system.

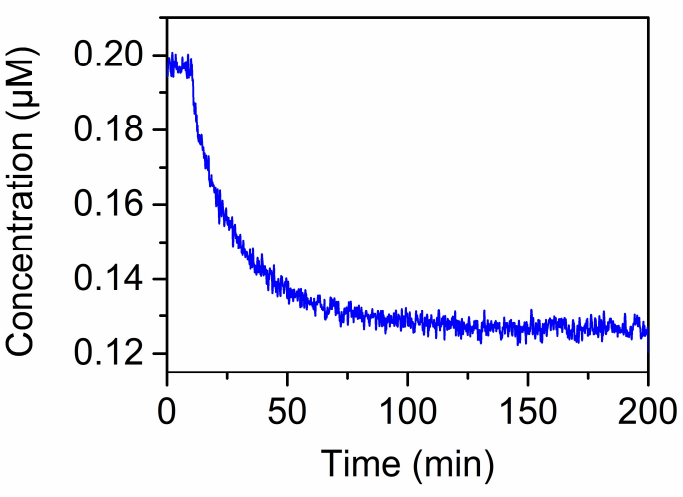

Figure S3. Control experiment where the A/B duplex and the strands Cy5-C and BHQ2-D are subjected to a modified trigger T_c, where the ribonucleobase in the substrate strand T is substituted by a DNA base. Under these conditions, the A/B scaffold is displaced by T_c, to yield the Pb^{2+}-ion-functionalized complex A/T_c and the product B/Cy5-C+BHQ2-D. Nonetheless, the A/T_c complex is catalytically inactive, resulting in only the depletion of the fluorescence of the system as a result of the formation of the B/Cy5-C+BHQ2-D, as shown in Fig. S3, but the dissipative recovery of the system is blocked, due to the formation of a catalytically inactive A/T_c DNAzyme. The result demonstrates that the formation of the Pb^{2+}-ion-dependent DNAzyme structure A/T is essential to drive the dissipative networks.

$$T + AB \underset{k_{-1}}{\overset{k_1}{\rightleftharpoons}} TA + B \quad (1)$$

$$B + C + D \underset{k_{-2}}{\overset{k_2}{\rightleftharpoons}} BCD \quad (2)$$

$$TA \xrightarrow{k_3} T_1T_2A \quad (3)$$

$$T_1T_2A \underset{k_{-4}}{\overset{k_4}{\rightleftharpoons}} T_1 + T_2 + A \quad (4)$$

$$A + BCD \underset{k_{-5}}{\overset{k_5}{\rightleftharpoons}} AB + C + D \quad (5)$$

$$AB \underset{k_{-6}}{\overset{k_6}{\rightleftharpoons}} A + B \quad (6)$$

Figure S4. Kinetic equations corresponding to the Pb^{2+}-ion-dependent DNAzyme-driven dissipative system shown in Fig. 1. The dissipative progress is followed by probing the fluorescence changes associated with B/Cy5-C+BHQ2-D.

$$\frac{dT}{dt} = -k_1[T][AB] + k_{-1}[TA][B]$$

$$\frac{dAB}{dt} = -k_1[T][AB] + k_{-1}[TA][B] + k_5[A][BCD] - k_{-5}[AB][C][D] - k_6[AB] + k_{-6}[A][B]$$

$$\frac{dTA}{dt} = k_1[T][AB] - k_{-1}[TA][B] - k_3[TA]$$

$$\frac{dB}{dt} = k_1[T][AB] - k_{-1}[TA][B] - k_2[B][C][D] + k_{-2}[BCD] + k_6[AB] - k_{-6}[A][B]$$

$$\frac{dC}{dt} = -k_2[B][C][D] + k_{-2}[BCD] + k_5[A][BCD] - k_{-5}[AB][C][D]$$

$$\frac{dD}{dt} = -k_2[B][C][D] + k_{-2}[BCD] + k_5[A][BCD] - k_{-5}[AB][C][D]$$

$$\frac{dBCD}{dt} = k_2[B][C][D] - k_{-2}[BCD] - k_5[A][BCD] + k_{-5}[AB][C][D]$$

$$\frac{dT_1T_2A}{dt} = k_3[TA] - k_4[T_1T_2A] + k_{-4}[T_1][T_2][A]$$

$$\frac{dT_1}{dt} = k_4[T_1T_2A] - k_{-4}[T_1][T_2][A]$$

$$\frac{dT_2}{dt} = k_4[T_1T_2A] - k_{-4}[T_1][T_2][A]$$

$$\frac{dA}{dt} = k_4[T_1T_2A] - k_{-4}[T_1][T_2][A] - k_5[A][BCD] + k_{-5}[AB][C][D] + k_6[AB] - k_{-6}[A][B]$$

Figure S5. Set of differential rate equations formulated to follow the kinetic model formulated in Fig. S4. This set of rate equations was applied to computationally simulate the contents of the B/Cy5-C+BHQ2-D module using the Matlab R2020a software to reach the best fit to the experimental results by non-linear least square optimization. The resulting computationally simulated rate constants of the best fit curves are summarized in Table S1.

Table S1. Computationally simulated rate constants for the Pb^{2+}-ion-dependent DNAzyme-driven networks shown in Fig. 1.

k_1	0.942 μM^{-1} min^{-1}	k_3	0.909 min^{-1}	k_{-5}	0.006 μM^{-2} min^{-1}
k_{-1}	83.522 μM^{-1} min^{-1}	k_4	96.832 min^{-1}	k_6	0.02145 min^{-1}
k_2	10.28 μM^{-2} min^{-1}	k_{-4}	44.409 μM^{-2} min^{-1}	k_{-6}	98.9 μM^{-1} min^{-1}
k_{-2}	0.0067 min^{-1}	k_5	2.31 μM^{-1} min^{-1}		

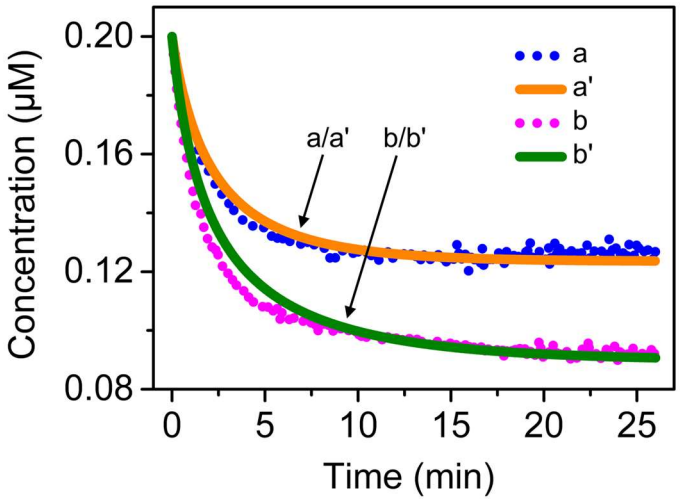

Figure S6. Experimental validation of the k_2/k_{-2} rate constants evaluated by the computational simulations. In this experiment constant concentrations of B, 0.2 μM, and Cy5-C, 0.2 μM, were subjected to two different concentrations of BHQ2-D, 0.08 μM, curve (a) and 0.12 μM, curve (b). The transient fluorescence changes of the Cy5 fluorophore as a result of the formation of the B/Cy5-C+BHQ2-D were followed. The two transient were kinetically modelled by the Matlab R2020a software and the values k_2/k_{-2} for the two curves were derived to be 10.42 μM^{-2} min^{-1} and 0.0068 min^{-1} that fits well with the computational simulation of the entire network, thus supporting the overall simulation of the dissipative system.

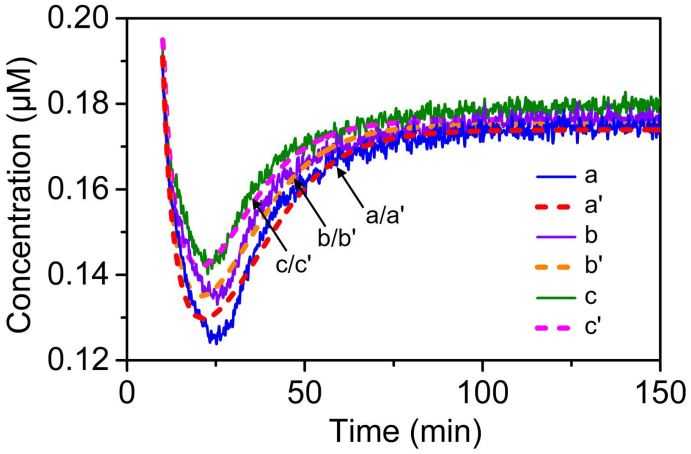

Figure S7. Dissipative transient curves for the separated Pb^{2+}-ion-dependent DNAzyme-driven network consisting of the A/B duplex, 0.2 μM, Pb^{2+} ions, 100 nM, the Cy3-E strand, 0.2 μM, and BHQ2-D strand, 0.2 μM. The dissipative transients (solid lines) are driven upon subjecting the network to the trigger T: (a) 1 μM, (b) 0.8 μM, (c) 0.6 μM. The dashed curves correspond to the computationally simulated results following the kinetic model shown in Fig. S9 and the set of differential rate equations formulated in Fig. S10.

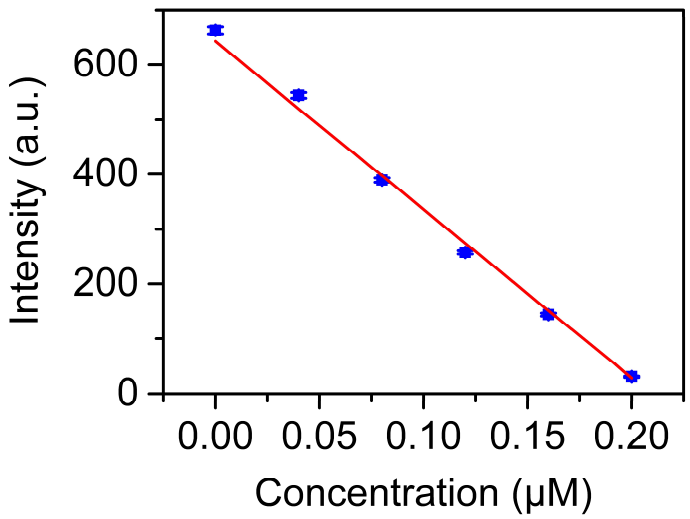

Figure S8. Calibration curve corresponding to the fluorescence intensities of a mixture of Cy3-E and BHQ2-D (each 0.2 μM) in the presence of variable concentrations of the strand B. The curve is fit linearly and the r^2 = 0.99641. The calibration curve provides a quantitative relation between the fluorescence intensity of the B/Cy3-E+BHQ2-D module and its molar concentration. The calibration curve provides a means to translate the fluorescence changes of the dissipative system into quantitative transient concentration changes of the reaction product B/Cy3-E+BHQ2-D along the dissipative transient operation of the system.

$$T + AB \underset{k_{-1}}{\overset{k_1}{\rightleftharpoons}} TA + B \quad (1)$$

$$B + E + D \underset{k_{-7}}{\overset{k_7}{\rightleftharpoons}} BED \quad (7)$$

$$TA \xrightarrow{k_3} T_1T_2A \quad (3)$$

$$T_1T_2A \underset{k_{-4}}{\overset{k_4}{\rightleftharpoons}} T_1 + T_2 + A \quad (4)$$

$$A + BED \underset{k_{-8}}{\overset{k_8}{\rightleftharpoons}} AB + E + D \quad (8)$$

$$AB \underset{k_{-6}}{\overset{k_6}{\rightleftharpoons}} A + B \quad (6)$$

Figure S9. Kinetic equations corresponding to the Pb^{2+}-ion-dependent DNAzyme-driven dissipative system. The dissipative progress is followed by probing the fluorescence changes associated with B/Cy3-E+BHQ2-D.

$$\frac{dT}{dt} = -k_1[T][AB] + k_{-1}[TA][B]$$

$$\frac{dAB}{dt} = -k_1[T][AB] + k_{-1}[TA][B] + k_8[A][BED] - k_{-8}[AB][E][D] - k_6[AB] + k_{-6}[A][B]$$

$$\frac{dTA}{dt} = k_1[T][AB] - k_{-1}[TA][B] - k_3[TA]$$

$$\frac{dB}{dt} = k_1[T][AB] - k_{-1}[TA][B] - k_7[B][E][D] + k_{-7}[BED] + k_6[AB] - k_{-6}[A][B]$$

$$\frac{dE}{dt} = -k_7[B][E][D] + k_{-7}[BED] + k_8[A][BED] - k_{-8}[AB][E][D]$$

$$\frac{dD}{dt} = -k_7[B][E][D] + k_{-7}[BED] + k_8[A][BED] - k_{-8}[AB][E][D]$$

$$\frac{dBED}{dt} = k_7[B][E][D] - k_{-7}[BED] - k_8[A][BED] + k_{-8}[AB][E][D]$$

$$\frac{dT_1T_2A}{dt} = k_3[TA] - k_4[T_1T_2A] + k_{-4}[T_1][T_2][A]$$

$$\frac{dT_1}{dt} = k_4[T_1T_2A] - k_{-4}[T_1][T_2][A]$$

$$\frac{dT_2}{dt} = k_4[T_1T_2A] - k_{-4}[T_1][T_2][A]$$

$$\frac{dA}{dt} = k_4[T_1T_2A] - k_{-4}[T_1][T_2][A] - k_8[A][BED] + k_{-8}[AB][E][D] + k_6[AB] - k_{-6}[A][B]$$

Figure S10. Set of differential rate equations formulated to follow the kinetic model formulated in Fig. S9. This set of rate equations was applied to computationally simulate the contents of the B/Cy3-E+BHQ2-D module using the Matlab R2020a software to reach the best fit to the experimental results by non-linear least square optimization. The resulting computationally simulated rate constants of the best fit curves are summarized in Table S2.

Table S2. Computationally simulated rate constants for the Pb^{2+}-ion-dependent DNAzyme-driven networks shown in Fig. S7.

k_1	0.942 μM^{-1} min^{-1}	k_{-4}	44.409 μM^{-2} min^{-1}	k_{-7}	0.0055 min^{-1}
k_{-1}	83.522 μM^{-1} min^{-1}	k_6	0.02145 min^{-1}	k_8	1.798 μM^{-1} min^{-1}
k_3	0.909 min^{-1}	k_{-6}	98.9 μM^{-1} min^{-1}	k_{-8}	0.0061 μM^{-2} min^{-1}
k_4	96.832 min^{-1}	k_7	10.5 μM^{-2} min^{-1}		

$$T + AB \underset{k_{-1}}{\overset{k_1}{\rightleftharpoons}} TA + B \quad (1)$$

$$B + C + D \underset{k_{-2}}{\overset{k_2}{\rightleftharpoons}} BCD \quad (2)$$

$$B + E + D \underset{k_{-7}}{\overset{k_7}{\rightleftharpoons}} BED \quad (7)$$

$$TA \xrightarrow{k_3} T_1T_2A \quad (3)$$

$$T_1T_2A \underset{k_{-4}}{\overset{k_4}{\rightleftharpoons}} T_1 + T_2 + A \quad (4)$$

$$A + BCD \underset{k_{-5}}{\overset{k_5}{\rightleftharpoons}} AB + C + D \quad (5)$$

$$A + BED \underset{k_{-8}}{\overset{k_8}{\rightleftharpoons}} AB + E + D \quad (8)$$

$$AB \underset{k_{-6}}{\overset{k_6}{\rightleftharpoons}} A + B \quad (6)$$

Figure S11. Kinetic equations corresponding to the Pb^{2+}-ion-dependent DNAzyme-driven competitive dissipative process consisting of the networks shown in Fig. 3, Panel I and II. The dissipative transients are recorded by probing the fluorescence changes of the B/Cy5-C+BHQ2-D and B/Cy3-E+BHQ2-D products.

$$\frac{dT}{dt} = -k_1[T][AB] + k_{-1}[TA][B]$$

$$\frac{dAB}{dt} = -k_1[T][AB] + k_{-1}[TA][B] + k_5[A][BCD] - k_{-5}[AB][C][D] + k_8[A][BED] - k_{-8}[AB][E][D] - k_6[AB] + k_{-6}[A][B]$$

$$\frac{dTA}{dt} = k_1[T][AB] - k_{-1}[TA][B] - k_3[TA]$$

$$\frac{dB}{dt} = k_1[T][AB] - k_{-1}[TA][B] - k_2[B][C][D] + k_{-2}[BCD] - k_7[B][E][D] + k_{-7}[BED] + k_6[AB] - k_{-6}[A][B]$$

$$\frac{dC}{dt} = -k_2[B][C][D] + k_{-2}[BCD] + k_5[A][BCD] - k_{-5}[AB][C][D]$$

$$\frac{dD}{dt} = -k_2[B][C][D] + k_{-2}[BCD] - k_7[B][E][D] + k_{-7}[BED] + k_5[A][BCD] - k_{-5}[AB][C][D] + k_8[A][BED] - k_{-8}[AB][E][D]$$

$$\frac{dE}{dt} = -k_7[B][E][D] + k_{-7}[BED] + k_8[A][BED] - k_{-8}[AB][E][D]$$

$$\frac{dBCD}{dt} = k_2[B][C][D] - k_{-2}[BCD] - k_5[A][BCD] + k_{-5}[AB][C][D]$$

$$\frac{dBED}{dt} = k_7[B][E][D] - k_{-7}[BED] - k_8[A][BED] + k_{-8}[AB][E][D]$$

$$\frac{dT_1T_2A}{dt} = k_3[TA] - k_4[T_1T_2A] + k_{-4}[T_1][T_2][A]$$

$$\frac{dT_1}{dt} = k_4[T_1T_2A] - k_{-4}[T_1][T_2][A]$$

$$\frac{dT_2}{dt} = k_4[T_1T_2A] - k_{-4}[T_1][T_2][A]$$

$$\frac{dA}{dt} = k_4[T_1T_2A] - k_{-4}[T_1][T_2][A] - k_5[A][BCD] + k_{-5}[AB][C][D] - k_8[A][BED] + k_{-8}[AB][E][D] + k_6[AB] - k_{-6}[A][B]$$

Figure S12. Set of differential rate equations formulated to follow the kinetic model shown in Fig. S11, corresponding to dissipative system consisting of two competitive networks, Cf. Fig. 3, Panel I and II.

$$T + AB \underset{k_{-1}}{\overset{k_1}{\rightleftharpoons}} TA + B \quad (1)$$

$$B + C + D \underset{k_{-2}}{\overset{k_2}{\rightleftharpoons}} BCD \quad (2)$$

$$B + E + D \underset{k_{-7}}{\overset{k_7}{\rightleftharpoons}} BED \quad (7)$$

$$TA \xrightarrow{k_3} T_1T_2A \quad (3)$$

$$T_1T_2A \underset{k_{-4}}{\overset{k_4}{\rightleftharpoons}} T_1 + T_2 + A \quad (4)$$

$$A + BCD \underset{k_{-5}}{\overset{k_5}{\rightleftharpoons}} AB + C + D \quad (5)$$

$$A + BED \underset{k_{-8}}{\overset{k_8}{\rightleftharpoons}} AB + E + D \quad (8)$$

$$AB \underset{k_{-6}}{\overset{k_6}{\rightleftharpoons}} A + B \quad (6)$$

$$C + I_1 \underset{k_{-9}}{\overset{k_9}{\rightleftharpoons}} CI_1 \quad (9)$$

Figure S13. Kinetic equations corresponding to the Pb^{2+}-ion-dependent DNAzyme-driven the gated dissipative system in the presence of inhibitor I_1, Cf. Fig. 3, Panel III and IV.

$$\frac{dT}{dt} = -k_1[T][AB] + k_{-1}[TA][B]$$

$$\frac{dAB}{dt} = -k_1[T][AB] + k_{-1}[TA][B] + k_5[A][BCD] - k_{-5}[AB][C][D] + k_8[A][BED] - k_{-8}[AB][E][D] - k_6[AB] + k_{-6}[A][B]$$

$$\frac{dTA}{dt} = k_1[T][AB] - k_{-1}[TA][B] - k_3[TA]$$

$$\frac{dB}{dt} = k_1[T][AB] - k_{-1}[TA][B] - k_2[B][C][D] + k_{-2}[BCD] - k_7[B][E][D] + k_{-7}[BED] + k_6[AB] - k_{-6}[A][B]$$

$$\frac{dC}{dt} = -k_2[B][C][D] + k_{-2}[BCD] + k_5[A][BCD] - k_{-5}[AB][C][D] - k_9[C][I_1] + k_{-9}[CI_1]$$

$$\frac{dD}{dt} = -k_2[B][C][D] + k_{-2}[BCD] - k_7[B][E][D] + k_{-7}[BED] + k_5[A][BCD] - k_{-5}[AB][C][D] + k_8[A][BED] - k_{-8}[AB][E][D]$$

$$\frac{dE}{dt} = -k_7[B][E][D] + k_{-7}[BED] + k_8[A][BED] - k_{-8}[AB][E][D]$$

$$\frac{dBCD}{dt} = k_2[B][C][D] - k_{-2}[BCD] - k_5[A][BCD] + k_{-5}[AB][C][D]$$

$$\frac{dBED}{dt} = k_7[B][E][D] - k_{-7}[BED] - k_8[A][BED] + k_{-8}[AB][E][D]$$

$$\frac{dT_1T_2A}{dt} = k_3[TA] - k_4[T_1T_2A] + k_{-4}[T_1][T_2][A]$$

$$\frac{dT_1}{dt} = k_4[T_1T_2A] - k_{-4}[T_1][T_2][A]$$

$$\frac{dT_2}{dt} = k_4[T_1T_2A] - k_{-4}[T_1][T_2][A]$$

$$\frac{dA}{dt} = k_4[T_1T_2A] - k_{-4}[T_1][T_2][A] - k_5[A][BCD] + k_{-5}[AB][C][D] - k_8[A][BED] + k_{-8}[AB][E][D] + k_6[AB] - k_{-6}[A][B]$$

$$\frac{dI_1}{dt} = -k_9[C][I_1] + k_{-9}[CI_1]$$

$$\frac{dCI_1}{dt} = k_9[C][I_1] - k_{-9}[CI_1]$$

Figure S14. Set of differential rate equations formulated to follow the kinetic model formulated in Fig. S13. This set of rate equations was applied to computationally simulate the contents of the B/Cy5-C+BHQ2-D and B/Cy3-E+BHQ2-D modules in the presence of the inhibitor I_1 using the Matlab R2020a software to reach the best fit to the experimental results by non-linear least square optimization. The resulting computationally simulated rate constants of the best fit curves are summarized in Table S3.

Table S3. Computationally simulated rate constants for the gated Pb^{2+}-ion-dependent DNAzyme-driven networks in the presence of the inhibitor I_1.

k_1	0.942 μM^{-1} min^{-1}	k_{-4}	44.409 μM^{-2} min^{-1}	k_{-7}	0.0055 min^{-1}
k_{-1}	83.522 μM^{-1} min^{-1}	k_5	2.31 μM^{-1} min^{-1}	k_8	1.798 μM^{-1} min^{-1}
k_2	10.28 μM^{-2} min^{-1}	k_{-5}	0.006 μM^{-2} min^{-1}	k_{-8}	0.0061 μM^{-2} min^{-1}
k_{-2}	0.0067 min^{-1}	k_6	0.02145 min^{-1}	k_9	93.5 μM^{-1} min^{-1}
k_3	0.909 min^{-1}	k_{-6}	98.9 μM^{-1} min^{-1}	k_{-9}	0.0032 min^{-1}
k_4	96.832 min^{-1}	k_7	10.5 μM^{-2} min^{-1}		

$$T + AB \underset{k_{-1}}{\overset{k_1}{\rightleftharpoons}} TA + B \quad (1)$$

$$B + C + D \underset{k_{-2}}{\overset{k_2}{\rightleftharpoons}} BCD \quad (2)$$

$$B + E + D \underset{k_{-7}}{\overset{k_7}{\rightleftharpoons}} BED \quad (7)$$

$$TA \xrightarrow{k_3} T_1T_2A \quad (3)$$

$$T_1T_2A \underset{k_{-4}}{\overset{k_4}{\rightleftharpoons}} T_1 + T_2 + A \quad (4)$$

$$A + BCD \underset{k_{-5}}{\overset{k_5}{\rightleftharpoons}} AB + C + D \quad (5)$$

$$A + BED \underset{k_{-8}}{\overset{k_8}{\rightleftharpoons}} AB + E + D \quad (8)$$

$$AB \underset{k_{-6}}{\overset{k_6}{\rightleftharpoons}} A + B \quad (6)$$

$$E + I_2 \underset{k_{-10}}{\overset{k_{10}}{\rightleftharpoons}} EI_2 \quad (10)$$

Figure S15. Kinetic equations corresponding to the Pb^{2+}-ion-dependent DNAzyme-driven the gated dissipative system in the presence of inhibitor I_2, Cf. Fig. 3, Panel V and VI.

$$\frac{dT}{dt} = -k_1[T][AB] + k_{-1}[TA][B]$$

$$\frac{dAB}{dt} = -k_1[T][AB] + k_{-1}[TA][B] + k_5[A][BCD] - k_{-5}[AB][C][D] + k_8[A][BED] - k_{-8}[AB][E][D] - k_6[AB] + k_{-6}[A][B]$$

$$\frac{dTA}{dt} = k_1[T][AB] - k_{-1}[TA][B] - k_3[TA]$$

$$\frac{dB}{dt} = k_1[T][AB] - k_{-1}[TA][B] - k_2[B][C][D] + k_{-2}[BCD] - k_7[B][E][D] + k_{-7}[BED] + k_6[AB] - k_{-6}[A][B]$$

$$\frac{dC}{dt} = -k_2[B][C][D] + k_{-2}[BCD] + k_5[A][BCD] - k_{-5}[AB][C][D]$$

$$\frac{dD}{dt} = -k_2[B][C][D] + k_{-2}[BCD] - k_7[B][E][D] + k_{-7}[BED] + k_5[A][BCD] - k_{-5}[AB][C][D] + k_8[A][BED] - k_{-8}[AB][E][D]$$

$$\frac{dE}{dt} = -k_7[B][E][D] + k_{-7}[BED] + k_8[A][BED] - k_{-8}[AB][E][D] - k_{10}[E][I_2] + k_{-10}[EI_2]$$

$$\frac{dBCD}{dt} = k_2[B][C][D] - k_{-2}[BCD] - k_5[A][BCD] + k_{-5}[AB][C][D]$$

$$\frac{dBED}{dt} = k_7[B][E][D] - k_{-7}[BED] - k_8[A][BED] + k_{-8}[AB][E][D]$$

$$\frac{dT_1T_2A}{dt} = k_3[TA] - k_4[T_1T_2A] + k_{-4}[T_1][T_2][A]$$

$$\frac{dT_1}{dt} = k_4[T_1T_2A] - k_{-4}[T_1][T_2][A]$$

$$\frac{dT_2}{dt} = k_4[T_1T_2A] - k_{-4}[T_1][T_2][A]$$

$$\frac{dA}{dt} = k_4[T_1T_2A] - k_{-4}[T_1][T_2][A] - k_5[A][BCD] + k_{-5}[AB][C][D] - k_8[A][BED] + k_{-8}[AB][E][D] + k_6[AB] - k_{-6}[A][B]$$

$$\frac{dI_2}{dt} = -k_{10}[E][I_2] + k_{-10}[EI_2]$$

$$\frac{dEI_2}{dt} = k_{10}[E][I_2] - k_{-10}[EI_2]$$

Figure S16. Set of differential rate equations formulated to follow the kinetic model formulated in Fig. S15. This set of rate equations was applied to computationally simulate the contents of the B/Cy5-C+BHQ2-D and B/Cy3-E+BHQ2-D modules in the presence of the inhibitor I_2 using the Matlab R2020a software to reach the best fit to the experimental results by non-linear least square optimization. The resulting computationally simulated rate constants of the best fit curves are summarized in Table S4.

Table S4. Computationally simulated rate constants for the gated Pb^{2+}-ion-dependent DNAzyme-driven networks in the presence of the inhibitor I_2.

k_1	0.942 μM^{-1} min^{-1}	k_{-4}	44.409 μM^{-2} min^{-1}	k_{-7}	0.0055 min^{-1}
k_{-1}	83.522 μM^{-1} min^{-1}	k_5	2.31 μM^{-1} min^{-1}	k_8	1.798 μM^{-1} min^{-1}
k_2	10.28 μM^{-2} min^{-1}	k_{-5}	0.006 μM^{-2} min^{-1}	k_{-8}	0.0061 μM^{-2} min^{-1}
k_{-2}	0.0067 min^{-1}	k_6	0.02145 min^{-1}	k_{10}	73.5 μM^{-1} min^{-1}
k_3	0.909 min^{-1}	k_{-6}	98.9 μM^{-1} min^{-1}	k_{-10}	0.00256 min^{-1}
k_4	96.832 min^{-1}	k_7	10.5 μM^{-2} min^{-1}		

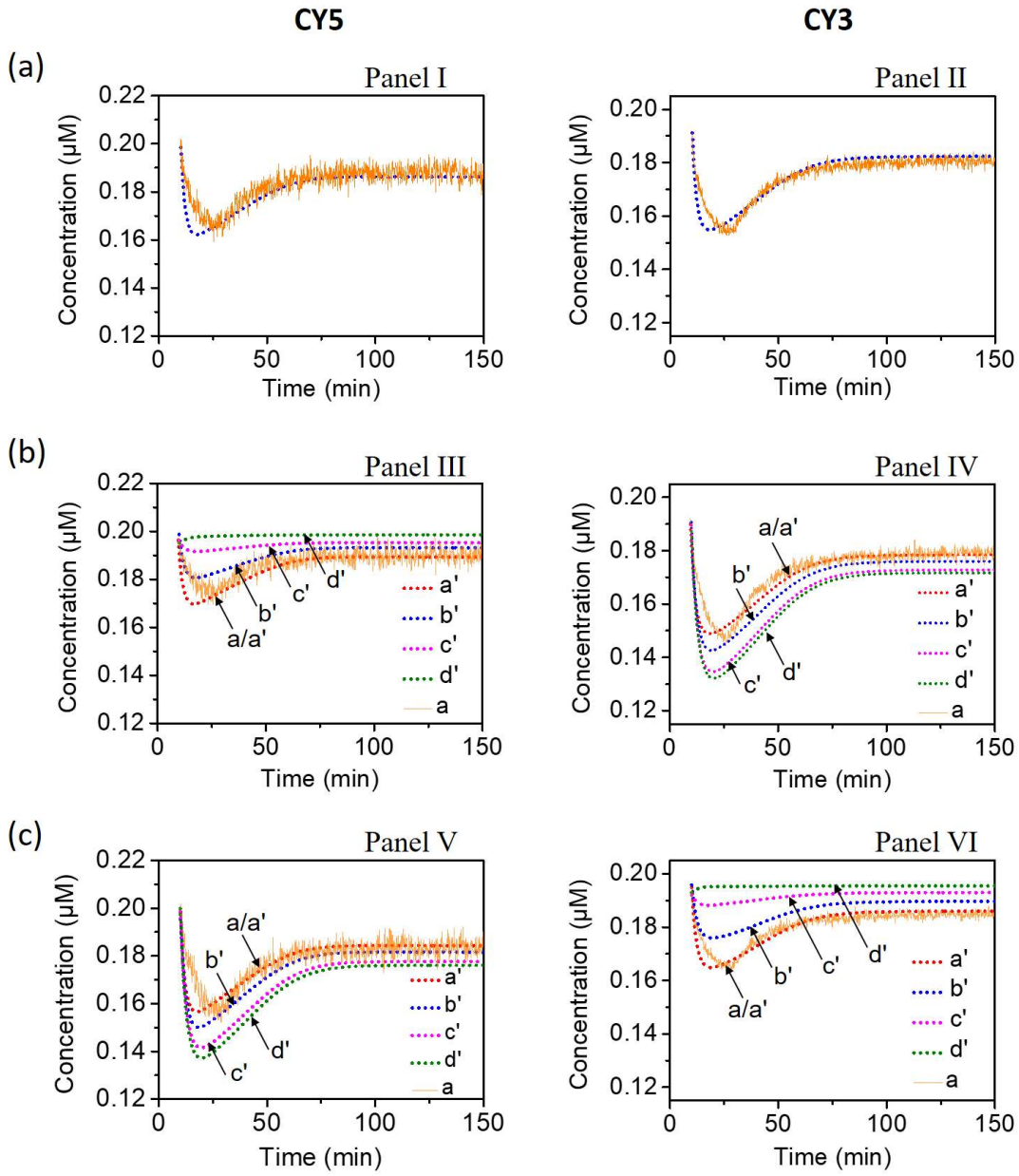

Figure S17. Computational simulated transients corresponding to the systems shown in Fig. 3 and the respective experimental results shown in Fig. 4. (a) Panel I and II present the computational simulated dissipative transients for the results shown in Fig. 4, Panel I and II. (b) Panel III and IV show the computational simulated transients corresponding to the inhibitor I_1 gated dissipative networks, Gate 1, shown in Fig. 4, Panel III and IV, in the presence of variable concentrations of I_1: (a/a', I_1 = 0.06 μM; b', I_1 = 0.12 μM; c', I_1 = 0.18 μM; d', I_1 = 0.2 μM). (c) Panel V and VI show the computational simulated transients corresponding to the inhibitor I_2 gated dissipative networks, Gate 2, shown in Fig. 4, Panel V and VI, in the presence of variable concentrations of I_2: (a/a', I_2 = 0.06 μM; b', I_2 = 0.12 μM; c', I_2 = 0.18 μM; d', I_2 = 0.2 μM). The solid lines correspond to the experimental results and the dashed lines are the computational simulated data.

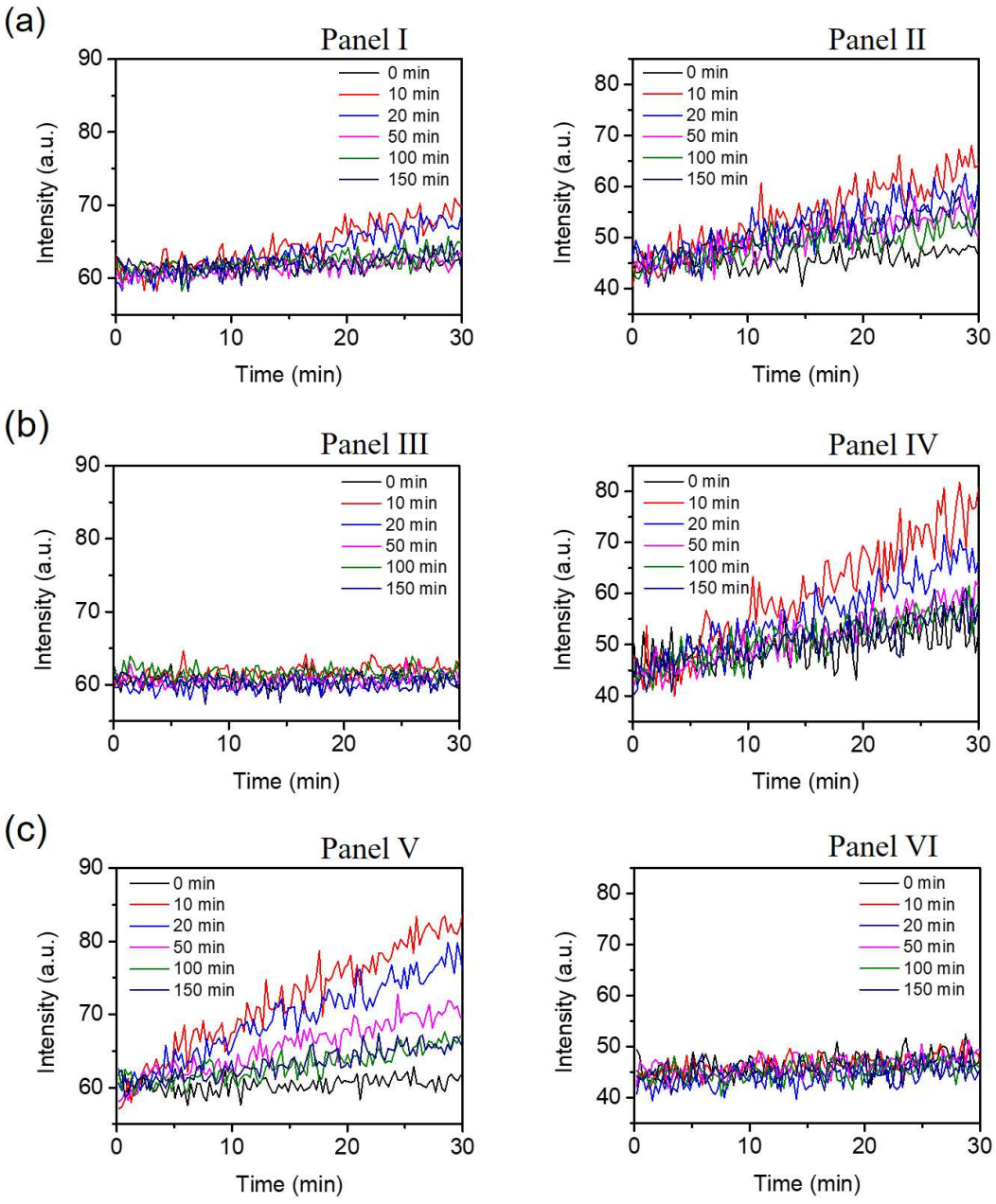

Figure S18: Rates corresponding to the cleavage of substrate S_1 and substrate S_2 by DNAzyme(1), Panels I and DNAzyme(2), Panels II, at different time of the transient processes corresponding to: (a) state "A" in Figure 6(a), (b) state "B", gated by I_1, Figure 6(b), (c) state "C" in Figure 6(c), gated by I_2.

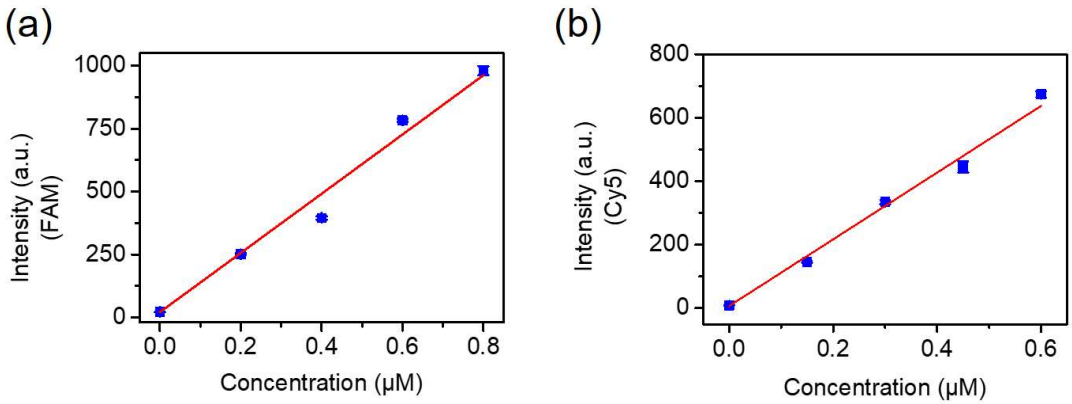

Figure S19: (a) Calibration curve corresponding to the fluorescence intensities of FAM-modified fragmented M at variable concentrations. The curve is fit linearly and the r^2 = 0.98402. (b) Calibration curve corresponding to the fluorescence intensities of Cy5-modified fragmented N at variable concentrations. The curve is fit linearly and the r^2 = 0.99095.

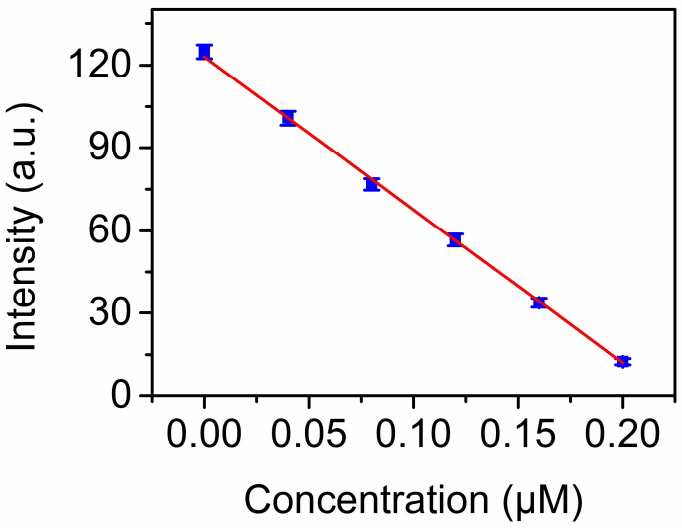

Figure S20. Calibration curve corresponding to the concentrations of the constituents H/Cy5-I in the presence of J/BHQ2-K to monitor the light-induced dissipative process shown in Fig. 7. The curve is fit linearly and the r^2 = 0.99922. The calibration curve is derived by applying a constant concentration of H/Cy5-I, 0.2 μM, and following the fluorescence changes (quenching) by the addition of variable concentrations of J/BHQ2-K.

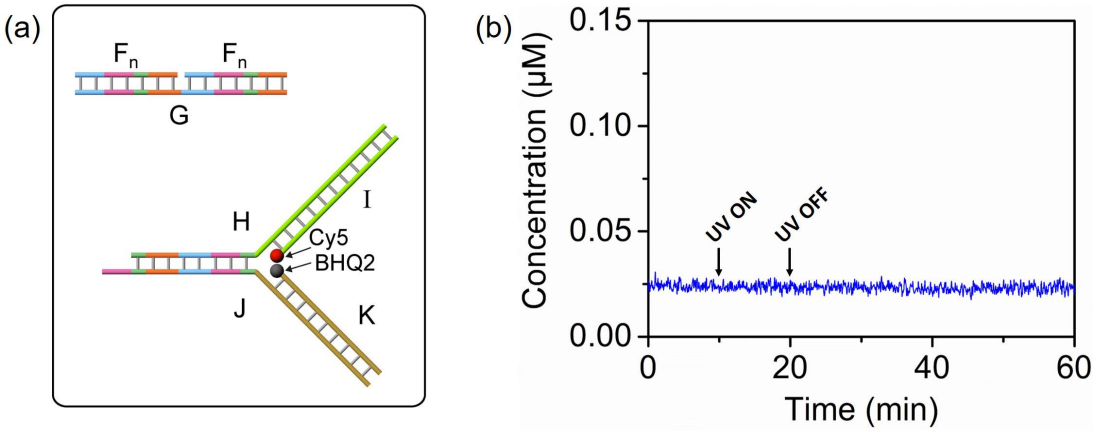

Figure S21. Control experiment verifying the need of the azobenzene functionalized G/$(F_t)_2$ duplex to drive the light-induced dissipative system. In this experiment, a duplex lacking the azobenzene functionalities, G/$(F_n)_2$ duplex is used, Fig. S21 (a). No dissipative process is observed upon UV irradiation of the system, Fig. S21 (b).

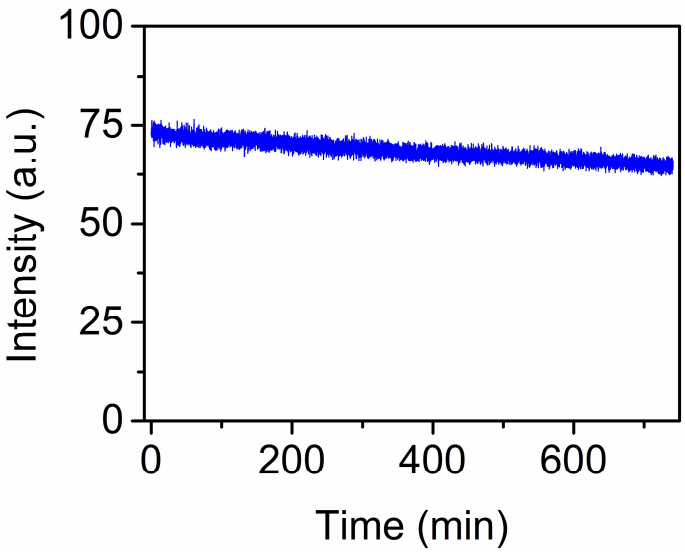

Figure S22. Control experiment confirming that the dissipative light-induced process shown in Fig. 7 requires a temperature of 55°C to induce the recovery of the original net. Fig. S22 shows the transient curve generated upon the UV irradiation of system at 55°C to generate the intermediate product H/Cy5-I and G/J/BHQ2-K followed by the immediate cooling of the system to 25°C. Very inefficient dissipative decay of the system is observed.

$$G(F_t)_2 \xrightarrow[k_{11}]{UV} G(F_c)_2 \quad (11)$$

$$G(F_c)_2 \underset{k_{-12}}{\overset{k_{12}}{\rightleftharpoons}} G + 2F_c \quad (12)$$

$$F_c \xrightarrow{k_{13}} F_t \quad (13)$$

$$F_t \xrightarrow[k_{14}]{UV} F_c \quad (14)$$

$$G + HIJK \underset{k_{-15}}{\overset{k_{15}}{\rightleftharpoons}} GJK + HI \quad (15)$$

$$2F_t + GJK \underset{k_{-16}}{\overset{k_{16}}{\rightleftharpoons}} G(F_t)_2 + JK \quad (16)$$

$$JK + HI \underset{k_{-17}}{\overset{k_{17}}{\rightleftharpoons}} HIJK \quad (17)$$

Figure S23. Kinetic equations corresponding to the UV light-driven dissipative system.

$$\frac{dG(F_t)_2}{dt} = -k_{11}[G(F_t)_2] + k_{16}[F_t]^2[GJK] - k_{-16}[G(F_t)_2][JK]$$

$$\frac{dG(F_c)_2}{dt} = k_{11}[G(F_t)_2] - k_{12}[G(F_c)_2] + k_{-12}[G][F_c]^2$$

$$\frac{dG}{dt} = k_{12}[G(F_c)_2] - k_{-12}[G][F_c]^2 - k_{15}[G][HIJK] + k_{-15}[GJK][HI]$$

$$\frac{dF_c}{dt} = k_{12}[G(F_c)_2] - k_{-12}[G][F_c]^2 - k_{13}[F_c] + k_{14}[F_t]$$

$$\frac{dF_t}{dt} = k_{13}[F_c] - k_{14}[F_t] - k_{16}[F_t]^2[GJK] + k_{-16}[G(F_t)_2][JK]$$

$$\frac{dHIJK}{dt} = -k_{15}[G][HIJK] + k_{-15}[GJK][HI] + k_{17}[JK][HI] - k_{-17}[HIJK]$$

$$\frac{dGJK}{dt} = k_{15}[G][HIJK] - k_{-15}[GJK][HI] - k_{16}[F_t]^2[GJK] + k_{-16}[G(F_t)_2][JK]$$

$$\frac{dHI}{dt} = k_{15}[G][HIJK] - k_{-15}[GJK][HI] - k_{17}[JK][HI] + k_{-17}[HIJK]$$

$$\frac{dJK}{dt} = k_{16}[F_t]^2[GJK] - k_{-16}[G(F_t)_2][JK] - k_{17}[JK][HI] + k_{-17}[HIJK]$$

Figure S24. Set of differential rate equations formulated to follow the kinetic model formulated in Fig. S23. This set of rate equations was applied to computationally simulate the contents of the Y-shaped structure module using the Matlab R2020a software to reach the best fit to the experimental results by non-linear least square optimization. The resulting computationally simulated rate constants of the best fit curves are summarized in Table S5.

Table S5. Rate constants derived from the computational simulation of the UV light-driven dissipative system.

k_{11}	0.18052 min^{-1}	k_{14}	17.2777 min^{-1}	k_{-16}	0.32344 μM^{-1} min^{-1}
k_{12}	15.25584 min^{-1}	k_{15}	7.44184 μM^{-1} min^{-1}	k_{17}	90.1532 μM^{-1} min^{-1}
k_{-12}	0.07168 μM^{-2} min^{1}	k_{-15}	5.48606 μM^{-1} min^{-1}	k_{-17}	0.03002 min^{-1}
k_{13}	0.0071 min^{-1}	k_{16}	58.93276 μM^{-2} min^{-1}		

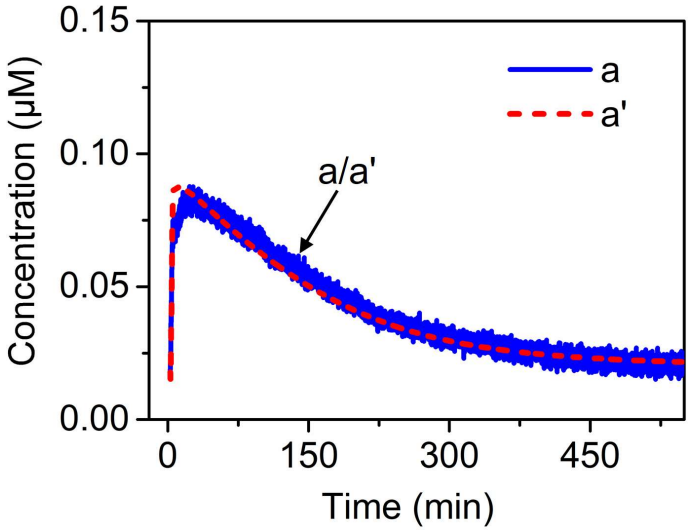

Figure S25. (a) Light-induced dissipative transient generated upon the illumination of the system shown in Fig. 7 for a time-interval of 5 min (in contrast to the experiment shown in Fig. 8(a) that applied of photoisomerization time-interval of 10 min). Evidently, the concentration of the intermediate products (H/Cy5-I and G/J/BHQ2-K is lower). The curve a' (dashed line) correspond to the computationally simulated fitting of curve a, using the rate constants derived in the primary simulation of the curves shown in Fig. 8(a) and the rate constants provided in Table S5, supporting the versatile fitting procedure (see, also Fig. S26).

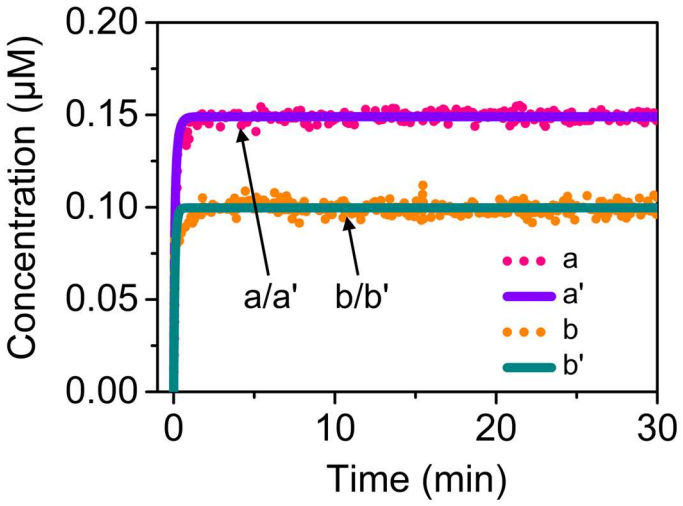

Figure S26. Experimental validation of the k_{17}/k_{-17} rate constants evaluated by the computational simulations. In this experiment constant concentrations of H, 0.2 μM, and I, 0.2 μM, were subjected to two different concentrations of J/K, 0.15 μM, curve (a) and 0.1 μM, curve (b). The transient fluorescence changes of the Cy5 fluorophore as a result of the formation of the Y-shaped structure were followed. The two transients were kinetically modelled by the Matlab R2020a software and the values k_{17}/k_{-17} for the two curves were derived to be 90.452 μM^{-1} min^{-1} and 0.0301 min^{-1} that fits well with the computational simulation of the entire network, thus supporting the overall simulation of the dissipative system.